

BI-TP 99/45  
LU-ITP 1999/020  
PSI-PR-99-29  
UR-1591  
hep-ph/9912261

# $\mathcal{O}(\alpha)$ corrections to $e^+e^- \rightarrow WW \rightarrow 4$ fermions(+ $\gamma$ ): first numerical results from RACOONWW

A. DENNER<sup>1</sup>, S. DITTMAYER<sup>2</sup>, M. ROTH<sup>3</sup> AND D. WACKEROTH<sup>4</sup>

<sup>1</sup> *Paul-Scherrer-Institut  
CH-5232 Villigen PSI, Switzerland*

<sup>2</sup> *Theoretische Physik, Universität Bielefeld  
D-33615 Bielefeld, Germany*

<sup>3</sup> *Institut für Theoretische Physik, Universität Leipzig  
D-04109 Leipzig, Germany*

<sup>4</sup> *Department of Physics, University of Rochester  
Rochester, NY 14627-0171, USA*

## **Abstract:**

First numerical results of the Monte Carlo generator RACOONWW for  $e^+e^- \rightarrow WW \rightarrow 4f(+\gamma)$  in the electroweak Standard Model are presented. This event generator is the first one that includes  $\mathcal{O}(\alpha)$  electroweak radiative corrections in the double-pole approximation completely. We briefly describe the strategy of the calculation and give numerical results for total cross sections, including CC03, and various distributions.

At present, the focus of Standard-Model (SM) tests lies on W-boson-pair production at LEP2, i.e. on the process  $e^+e^- \rightarrow WW \rightarrow 4f$ . In order to match the experimental accuracy of roughly 1%, theoretical predictions for the cross sections of  $e^+e^- \rightarrow 4f$  with a precision at or below the per-cent level are needed. This requires to include the complete set of lowest-order diagrams for  $e^+e^- \rightarrow 4f$  and the  $\mathcal{O}(\alpha)$  corrections to the W-pair production channels  $e^+e^- \rightarrow WW \rightarrow 4f$ . Since the impact of electroweak corrections grows with increasing energy, this task is even more important for future linear colliders with higher energy and luminosity.

In all regions of phase space where W-pair production dominates the cross section for  $e^+e^- \rightarrow 4f$ , an expansion of the matrix element about the poles of the resonant W propagators provides a reasonable approximation for the radiative corrections. Neglecting corrections to the non-doubly-resonant contributions leads to uncertainties of the order  $\alpha/\pi \times \Gamma_W/M_W \times \log(\dots) \sim 0.1\%$  with respect to the leading lowest-order contributions, where the logarithm indicates possible logarithmic enhancements. Thus, this so-called double-pole approximation (DPA) should be sufficient for an accuracy of 0.5% for observables that are dominated by doubly-resonant diagrams. Moreover, the DPA provides a gauge-invariant answer and allows us to use the existing results for on-shell W-pair production [ 1, 2] and W-boson decay [ 3, 4], as far as the virtual corrections are concerned.

The DPA for  $\mathcal{O}(\alpha)$  corrections to pair production of unstable particles has already been used in the literature. A possible strategy has been proposed in Ref. [ 5]. A Monte Carlo generator including the corrections to the W-pair production subprocess and the leading-logarithmic corrections to the W-boson decays has been constructed Refs. [ 6, 7], but non-factorizable corrections and W-spin correlations have been neglected there. A first complete calculation of the  $\mathcal{O}(\alpha)$  corrections for off-shell W-pair production, including a numerical study of leptonic final states, was presented in Ref. [ 8] using a semi-analytical approach, which is, however, only applicable to ideal theoretical situations.

In this paper we present the first complete calculation of the  $\mathcal{O}(\alpha)$  corrections for off-shell W-pair production in DPA that has been implemented in a Monte Carlo generator, which is called RACOONWW. This generator includes the complete lowest-order matrix elements for  $e^+e^- \rightarrow 4f$  for any four-fermion final state. For the virtual corrections a DPA is used without any additional approximations. In particular, the exact four-fermion phase space is used throughout. The virtual corrections consist of factorizable and non-factorizable contributions. The former are the ones that are associated to either W-pair production or W-boson decay; the results of Refs. [ 1, 3] are used in this part. The latter comprise all corrections in which the subprocesses production and decays do not proceed independently. Up to some simple supplements, the virtual non-factorizable corrections can be read off from the literature [ 9, 10]; we made use of the results of Ref. [ 10]. The real bremsstrahlung corrections are based on the full matrix-element calculation for  $e^+e^- \rightarrow 4f\gamma$  described in Ref. [ 11]. More precisely, the minimal gauge-invariant subset including all doubly-resonant contributions of the processes  $e^+e^- \rightarrow WW \rightarrow 4f\gamma$ , i.e. the photon radiation from the CC11 subset, are included. By using the exact matrix elements for the real radiation, we avoid problems in defining a DPA for semi-soft photons ( $E_\gamma \sim \Gamma_W$ ) and, moreover, can include the leading logarithmic corrections to non-doubly-resonant diagrams (background diagrams) exactly. The real corrections and the virtual corrections

are matched in such a way that all infrared singularities cancel exactly. The initial-state collinear singularities are regularized by retaining a finite electron mass and factorized into lowest-order matrix element and splitting functions. The collinear singularities connected to final-state radiation are treated inclusively, i.e. photons within collinear cones around the final-state fermions are integrated over, so that no logarithmic final-state fermion mass dependence survives. All contributions have been implemented in two programs, one of which uses the subtraction method described in Ref. [ 12], the other one uses phase-space slicing. All parts of the calculations have been performed in two independent ways. A detailed description of the calculation and the Monte Carlo generator RACOONWW will be published elsewhere [ 13].

For the numerical results we used the fixed-width scheme and the following parameters:

$$\begin{aligned}
G_\mu &= 1.16637 \times 10^{-5} \text{ GeV}^{-2}, & \alpha &= 1/137.0359895, \\
M_W &= 80.35 \text{ GeV}, & \Gamma_W &= 2.08699 \dots \text{ GeV}, \\
M_Z &= 91.1867 \text{ GeV}, & \Gamma_Z &= 2.49471 \text{ GeV}, \\
m_t &= 174.17 \text{ GeV}, & M_H &= 150 \text{ GeV}, \\
m_e &= 510.99907 \text{ keV}. & &
\end{aligned}
\tag{1}$$

The weak mixing angle is fixed by  $c_w = M_W/M_Z$ ,  $s_w^2 = 1 - c_w^2$ . These parameters are over-complete but self-consistent. Instead of  $\alpha$  we use  $G_\mu$  to parametrize the lowest-order matrix element, i.e. we use the effective coupling

$$\alpha_{G_\mu} = \frac{\sqrt{2}G_\mu M_W^2 s_w^2}{\pi}
\tag{2}$$

in the lowest-order matrix element. This parameterization has the advantage that all higher-order contributions associated with the running of the electromagnetic coupling and the leading universal two-loop  $m_t$ -dependent corrections are correctly taken into account. In the relative  $\mathcal{O}(\alpha)$  corrections, on the other hand, we use  $\alpha$ , since in the real corrections the scale of the real photon is zero. The W-boson width given above is calculated including the electroweak and QCD one-loop corrections with  $\alpha_s = 0.119$ . We do not include QCD corrections to the process  $e^+e^- \rightarrow WW \rightarrow 4f$ , and initial-state radiation is only taken into account in  $\mathcal{O}(\alpha)$ .

In Tables 1, 2, and 3 we present numbers for total cross sections without any cuts, for centre-of-mass (CM) energies 184, 189, and 200 GeV, respectively, based on 20 million events. In particular, we give the CC03 cross sections, i.e. the cross sections resulting from the signal diagrams only (defined in the 't Hooft–Feynman gauge). We also give numbers resulting from the complete set of diagrams for those final states where this is possible without cuts, i.e. the CC11 class of processes. In the considered cases, the effects of the background diagrams are below 0.2%. Note that we treat the external fermions as massless. Therefore, the cross sections for processes not in CC11 class become singular if no cuts are imposed for final-state electrons collinear to the beams and for virtual photons splitting into  $f\bar{f}$  pairs with small invariant masses. The shown corrections are typically  $-13\%$ ,  $-12\%$ , and  $-9\%$  at 184, 189, and 200 GeV, respectively. The numbers in parentheses are estimates of the Monte Carlo integration errors. The numbers for the

final state	CC03 Born	full Born	CC03 corrected	full corrected
$\nu_\mu\mu^+\tau^-\bar{\nu}_\tau$	210.26(5)	210.57(5)	182.21(11)	182.53(11)
$\nu_\mu\mu^+\text{d}\bar{\text{u}}$	630.8(2)	631.8(2)	546.5(3)	547.4(3)
$\text{u}\bar{\text{d}}\bar{\text{s}}\bar{\text{c}}$	1892.3(5)	1895.4(5)	1637.7(7)	1640.7(7)
total	17031(3)		14749(5)	

Table 1: Total cross sections in fb for  $e^+e^- \rightarrow WW \rightarrow 4f$  without cuts for various final states at 184 GeV

final state	CC03 Born	full Born	CC03 corrected	full corrected
$\nu_\mu\mu^+\tau^-\bar{\nu}_\tau$	216.07(6)	216.39(6)	190.64(11)	190.96(11)
$\nu_\mu\mu^+\text{d}\bar{\text{u}}$	648.2(2)	649.2(2)	571.6(3)	572.6(3)
$\text{u}\bar{\text{d}}\bar{\text{s}}\bar{\text{c}}$	1944.7(5)	1947.7(5)	1713.4(8)	1716.4(8)
total	17501(3)		15429(5)	

Table 2: Total cross sections in fb for  $e^+e^- \rightarrow WW \rightarrow 4f$  without cuts for various final states at 189 GeV

final state	CC03 Born	full Born	CC03 corrected	full corrected
$\nu_\mu\mu^+\tau^-\bar{\nu}_\tau$	219.82(6)	220.06(6)	199.74(12)	199.98(12)
$\nu_\mu\mu^+\text{d}\bar{\text{u}}$	659.5(2)	660.2(2)	598.9(3)	599.7(3)
$\text{u}\bar{\text{d}}\bar{\text{s}}\bar{\text{c}}$	1978.4(5)	1980.8(5)	1795.0(9)	1797.4(9)
total	17806(3)		16164(5)	

Table 3: Total cross sections in fb for  $e^+e^- \rightarrow WW \rightarrow 4f$  without cuts for various final states at 200 GeV

total W-pair production cross section in the last row of the tables directly result from the other rows by multiplying these with the number of equivalent channels and adding them up.

Next, we study various angular distributions. Here we restrict ourselves to the  $\nu_\mu\mu^+\text{d}\bar{\text{u}}$  final state and to  $\sqrt{s} = 200$  GeV. Because of our treatment of mass singularities (see Ref. [13] for details) it is necessary to combine photons that are collinear to the incoming or outgoing fermions appropriately with these fermions in order to obtain well-defined finite distributions. To this end we introduce the following recombination and cut procedure which proceeds in three steps:

1. All photons within a cone of 5 degrees around the beams are treated as invisible, i.e. their momenta are disregarded when calculating angles, energies, and invariant masses.

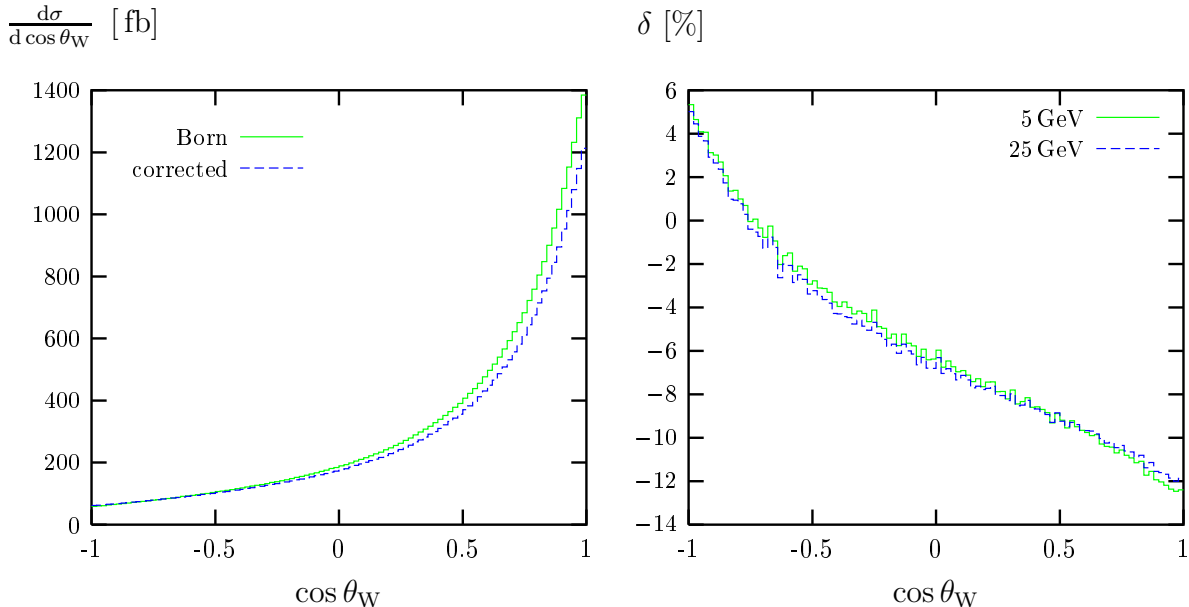


Figure 1: Production-angle distribution for  $e^+e^- \rightarrow \nu_\mu\mu^+d\bar{u}$  and  $\sqrt{s} = 200$  GeV

2. Next, the invariant masses of the photon with each of the charged final-state fermions are calculated. If the smallest one is smaller than  $M_{\text{rec}}$ , the photon is combined with the corresponding fermion, i.e. the momenta of the photon and the fermion are added and associated with the momentum of the fermion, and the photon is discarded.
3. Finally, all events are discarded in which one of the final-state fermions is within a cone of 10 degrees around the beams. No other cuts are applied.

We consider the cases of a tight recombination cut  $M_{\text{rec}} = 5$  GeV and of a loose recombination cut  $M_{\text{rec}} = 25$  GeV. In the following observables, the momenta of the W bosons are always defined by the sum of the momenta of the two corresponding decay fermions after the eventual recombination with the photon.

The results for the distributions have been obtained from 50 million events. In the following figures we always show on the left-hand side the absolute distributions in lowest order and including the corrections for the recombination cut  $M_{\text{rec}} = 5$  GeV, and on the right-hand side the corresponding relative corrections for the two recombination cuts  $M_{\text{rec}} = 5$  GeV and  $M_{\text{rec}} = 25$  GeV.

In Figure 1 we show the distribution of events in the angle between the  $W^+$  and the incoming  $e^+$ . Apart from the normalization effects, a distortion of the distribution occurs. This is mainly due to hard-photon emission from the initial state, which boosts the CM-system of the W bosons and causes a migration of events from regions with large cross section in the CM system to regions with small cross section in the laboratory system. This effect is also visible in the following distributions. The production-angle distribution hardly depends on the recombination scheme, as expected. An increase of the recombination cut leads to a small redistribution of events from the backward to the forward direction.

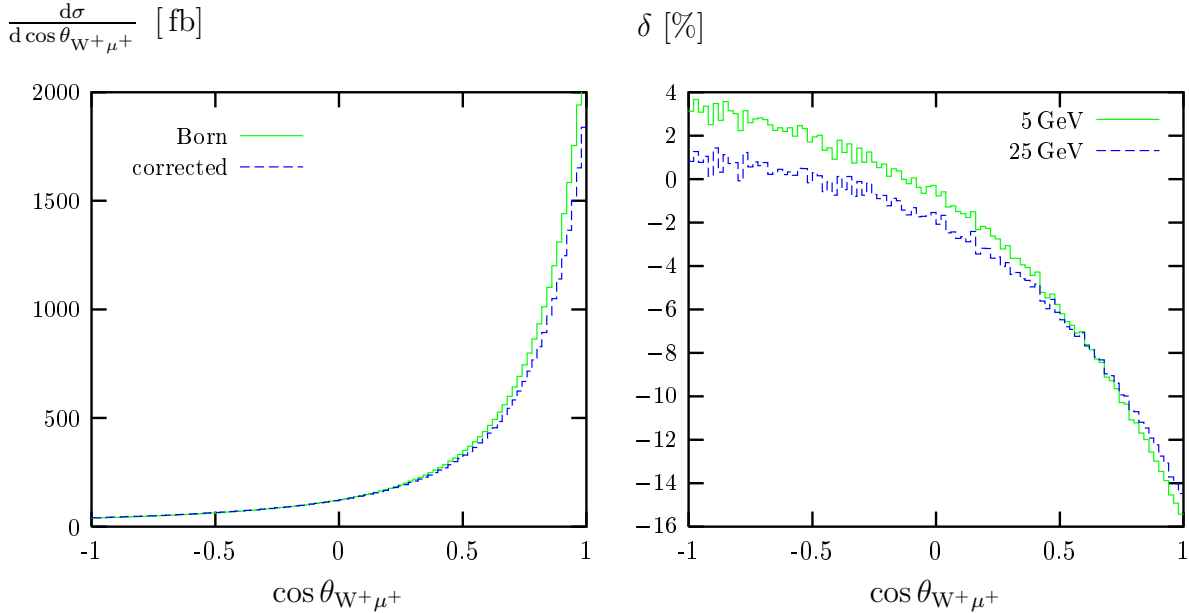


Figure 2: Decay-angle distribution for  $e^+e^- \rightarrow \nu_\mu\mu^+d\bar{u}$  and  $\sqrt{s} = 200$  GeV

The distribution of events in the angle between the  $W^+$  and the outgoing  $\mu^+$  is presented in Figure 2. In this case we find a sizeable dependence on the recombination mass  $M_{\text{rec}}$  for large decay angles, where the cross section is small. This originates from the fact that the recombination of a fermion with a photon parallel to this fermion decreases the angle between the fermion and the  $W$  boson from which the fermion results.

The distribution of events in the energy  $E_\mu$  of the outgoing  $\mu^+$  is depicted in Figure 3. In the on-shell approximation it would be restricted between  $20.2 \text{ GeV} < E_\mu < 79.8 \text{ GeV}$ . Outside this region, the corrections calculated in DPA are not reliable. The recombination of a photon with the muon increases the muon energy. Consequently, an increase of the recombination mass  $M_{\text{rec}}$  shifts the distribution to larger muon energies as can be seen in the relative corrections.

Finally, in Figures 4 and 5 we show the distributions of events in the invariant masses of the final-state lepton pair,  $M_{\mu\nu_\mu}$ , and of the final-state quark pair,  $M_{d\bar{u}}$ . The dependence on the recombination cut is sizeable everywhere. The results for the invariant-mass distributions can be understood as follows. For small recombination cuts, in most of the events the  $W$  bosons are defined from the decay fermions only. If a photon is emitted from the decay fermions and not recombined, the invariant mass of the fermions is smaller than the one of the decaying  $W$  boson. This leads to an enhancement of the distribution for invariant masses below the  $W$  resonance. This effect becomes smaller with increasing recombination mass. The enhancement is proportional to the squared charges of the final-state fermion, i.e. it is largest for the leptonic invariant mass. On the other hand, if the recombination mass gets large, the probability increases that the recombined fermion momenta receive contributions from photons that are radiated during the  $W$ -production subprocess or from the decay fermions of the other  $W$  boson. This leads to positive corrections above the considered  $W$  resonance. The effect is larger for the hadronic invariant mass since in this case, two decay fermions (the two quarks) can be combined with the

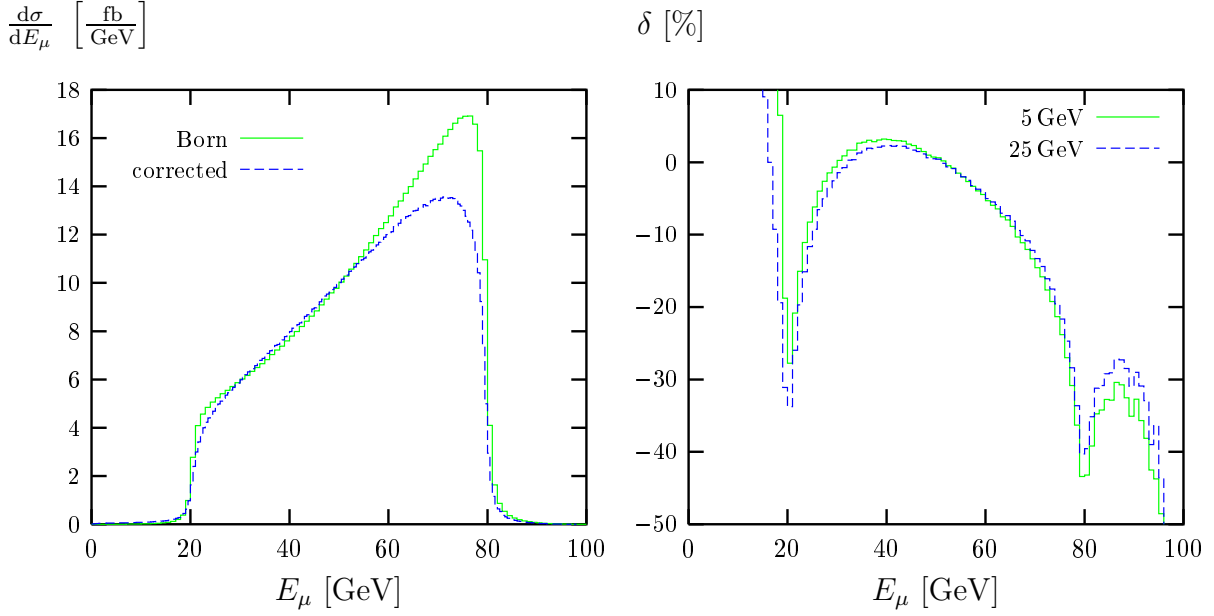


Figure 3: Muon-energy distribution for  $e^+e^- \rightarrow \nu_\mu\mu^+d\bar{u}$  and  $\sqrt{s} = 200$  GeV

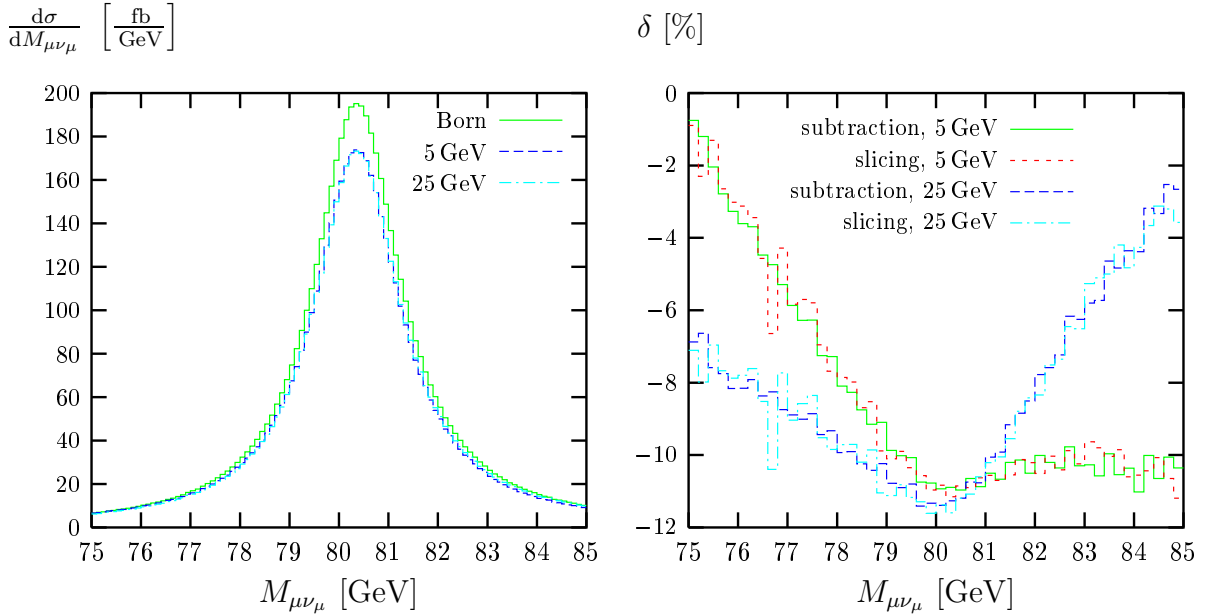


Figure 4: Invariant-mass distribution of the lepton pair for  $e^+e^- \rightarrow \nu_\mu\mu^+d\bar{u}$  and  $\sqrt{s} = 200$  GeV

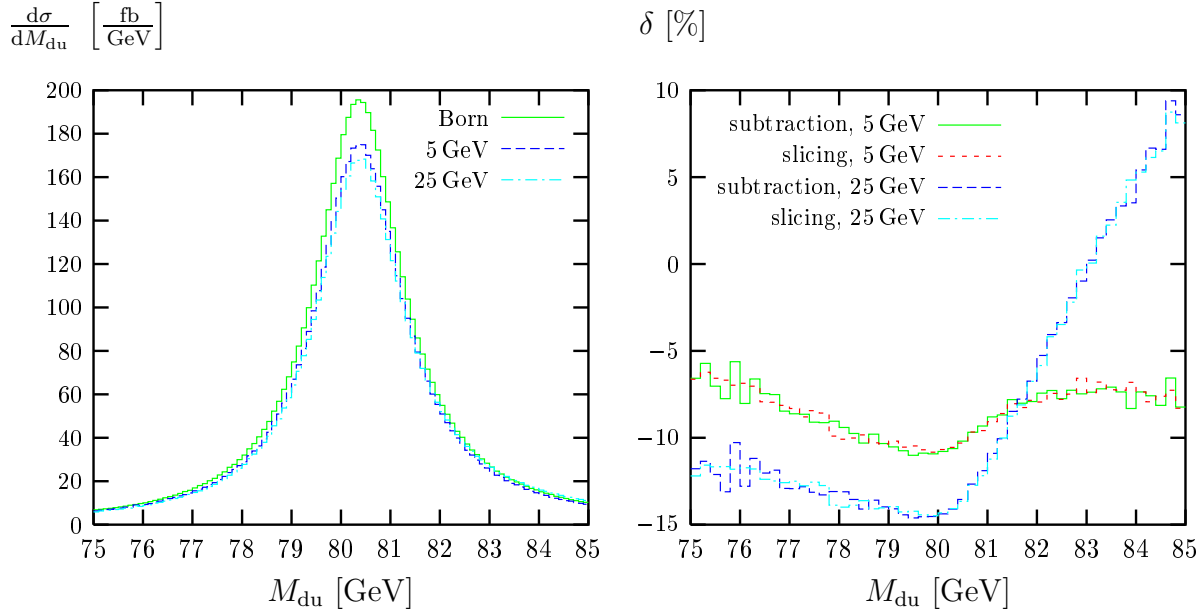


Figure 5: Invariant-mass distribution of the quark pair for  $e^+e^- \rightarrow \nu_\mu\mu^+d\bar{u}$  and  $\sqrt{s} = 200$  GeV

photon. The effect of the squared charges of the final-state fermions is marginal in this case because the contribution of initial-state fermions dominates.

The distortion of the W invariant-mass distributions is of particular interest for the reconstruction of the W-boson mass  $M_W$  from the decay products. In order to illustrate the impact of the corrections on the determination of  $M_W$ , we fit the simple Breit–Wigner distribution

$$\left(\frac{d\sigma}{dM^2}\right) = \frac{\text{const.}}{(M^2 - M_{W,\text{fit}}^2)^2 + M_{W,\text{fit}}^2 \Gamma_{W,\text{fit}}^2} \quad (3)$$

to the W line shapes shown in Figures 4 and 5, treating  $M_{W,\text{fit}}$  and  $\Gamma_{W,\text{fit}}$  (as well as the normalization constant) as free fit parameters. We determine the fitted W-boson masses from the predictions resulting from the lowest-order CC03 diagrams,  $M_{W,\text{fit}}^{\text{Born,CC03}}$ , from the complete lowest-order diagrams,  $M_{W,\text{fit}}^{\text{Born}}$ , and from the fully corrected predictions,  $M_{W,\text{fit}}^{\text{corr}}$ . In addition we give the mass shift resulting from the corrections  $\Delta M_{W,\text{fit}}^{\text{corr}} = M_{W,\text{fit}}^{\text{corr}} - M_{W,\text{fit}}^{\text{Born}}$ . The results of these fits, which are contained in Table 4, show that the fitted W-boson mass changes at the order of some 10 MeV if the corrections are included. From the discussion of the line-shape distortion above it is clear that this mass shift is more positive if more photons are recombined. The results also illustrate that the fit results vary at the order of some 10 MeV for different fit ranges in  $M$ .

We have also considered the case where each photon is recombined with the nearest fermion, i.e.  $M_{\text{rec}} > \sqrt{s}$ . In the distributions of the production angle, the decay angle, and the muon energy this increase of the recombination cut leads to the expected small changes of the corrections. For the invariant-mass distributions, the case of complete recombination differs from the case  $M_{\text{rec}} = 25$  GeV only by a slight decrease of the relative corrections. This is due to the fact that the recombination of a photon that forms an invariant mass of at least 25 GeV with charged fermions shifts the events by at least



	$M_{\text{rec}}$ [GeV]	$M_{\text{W,fit}}^{\text{Born,CC03}}$ [GeV]	$M_{\text{W,fit}}^{\text{Born}}$ [GeV]	$M_{\text{W,fit}}^{\text{corr}}$ [GeV]	$\Delta M_{\text{W,fit}}^{\text{corr}}$ [MeV]
$W^+ \rightarrow \nu_\mu \mu^+$	5	80.366	80.365	80.363	-2
		80.372	80.371	80.365	-5
	25	80.366	80.365	80.374	+9
		80.372	80.371	80.385	+14
$W^- \rightarrow d\bar{u}$	5	80.365	80.364	80.378	+14
		80.371	80.370	80.384	+14
	25	80.365	80.364	80.397	+32
		80.371	80.370	80.415	+46

Table 4: Results for  $M_{\text{W,fit}}$  for a Breit–Wigner fit to the invariant-mass distributions shown in Figures 4 and 5, using the fit ranges  $78.3 \text{ GeV} < M < 82.3 \text{ GeV}$  (upper values) and  $76.3 \text{ GeV} < M < 84.3 \text{ GeV}$  (lower values)

3.8 GeV for the leptonically-decaying W boson and 7.4 GeV for the hadronically-decaying W boson. Such a shift leads to an increase of the corrections only outside the range shown in Figures 4 and 5. Since there is no change in the shape of the distribution near the resonance, the results for the invariant-mass fit are essentially equivalent.

In the plots on the right-hand side in Figures 4 and 5 we have included the results for phase-space slicing and for the subtraction method. The agreement between these results demonstrates the correctness of our implementations and gives another estimate on the size of the integration errors.

In summary, we have constructed the event generator RACOONWW for  $e^+e^- \rightarrow WW \rightarrow 4f(+\gamma)$  which includes the complete  $\mathcal{O}(\alpha)$  electroweak corrections in double-pole approximation. With this generator we have calculated the total cross sections, including the CC03 cross sections, and various distributions of experimental relevance for typical LEP2 energies. The detailed numerical discussion of the corrections, in particular, illustrates the importance of the issue of photon recombination. More details of the RACOONWW approach and further results, including a comparison to results of other authors, will be presented elsewhere [13].

## References

- [1] M. Böhm et al., *Nucl. Phys.* **B304** (1988) 463.
- [2] J. Fleischer, F. Jegerlehner and M. Zralek, *Z. Phys.* **C42** (1989) 409.
- [3] A. Denner and T. Sack, *Z. Phys.* **C46** (1990) 653.
- [4] D.Yu. Bardin, S. Riemann and T. Riemann, *Z. Phys.* **C32** (1986) 121;  
F. Jegerlehner, *Z. Phys.* **C32** (1986) 425.
- [5] A. Aeppli, G.J. van Oldenborgh and D. Wyler, *Nucl. Phys.* **B428** (1994) 126.

- [6] S. Jadach et al., *Phys. Lett.* **B417** (1998) 326.
- [7] S. Jadach et al., hep-ph/9907436.
- [8] W. Beenakker, F.A. Berends and A.P. Chapovsky, *Nucl. Phys.* **B548** (1999) 3.
- [9] K. Melnikov and O.I. Yakovlev, *Nucl. Phys.* **B471** (1996) 90;  
W. Beenakker, A.P. Chapovsky and F.A. Berends, *Phys. Lett.* **B411** (1997) 203 and  
*Nucl. Phys.* **B508** (1997) 17.
- [10] A. Denner, S. Dittmaier and M. Roth, *Nucl. Phys.* **B519** (1998) 39 and *Phys. Lett.*  
**B429** (1998) 145.
- [11] A. Denner, S. Dittmaier, M. Roth and D. Wackerroth, *Nucl. Phys.* **B560** (1999) 33.
- [12] S. Dittmaier, BI-TP 99/09, hep-ph/9904440, to appear in *Nucl. Phys.* **B**;  
M. Roth, dissertation ETH Zürich No. 13363, 1999.
- [13] A. Denner, S. Dittmaier, M. Roth and D. Wackerroth, in preparation.